AGU PUBLICATIONS

Water Resources Research

RESEARCH ARTICLE
10.1002/2013WR015002

A significant nexus: Geographically isolated wetlands influence landscape hydrology

Daniel L. McLaughlin[1,2], David A. Kaplan[3], and Matthew J. Cohen[1]

[1]School of Forest Resources and Conservation, University of Florida, Gainesville, Florida, USA, [2]Now at Department of Forest Resources and Environmental Conservation, Virginia Polytechnic Institute and State University, Blacksburg, Virginia, USA, [3]Department of Environmental Engineering Sciences, University of Florida, Gainesville, Florida, USA

Key Points:
- GIWs act as hydrologic sinks and sources in response to climate
- GIWs effects on regional water table and base flow were modeled
- GIWs buffer surficial aquifer variation, impacting stream base flow

Correspondence to:
D. L. McLaughlin,
mclaugd@vt.edu

Citation:
McLaughlin, D. L., D. A. Kaplan, and M. J. Cohen (2014), A significant nexus: Geographically isolated wetlands influence landscape hydrology, *Water Resour. Res.*, *50*, doi:10.1002/2013WR015002.

Received 5 NOV 2013
Accepted 15 AUG 2014
Accepted article online 19 AUG 2014

Abstract Recent U.S. Supreme Court rulings have limited federal protections for geographically isolated wetlands (GIWs) except where a "significant nexus" to a navigable water body is demonstrated. Geographic isolation does not imply GIWs are hydrologically disconnected; indeed, wetland-groundwater interactions may yield important controls on regional hydrology. Differences in specific yield (S_y) between uplands and inundated GIWs drive differences in water level responses to precipitation and evapotranspiration, leading to frequent reversals in hydraulic gradients that cause GIWs to act as both groundwater sinks and sources. These reversals are predicted to buffer surficial aquifer dynamics and thus base flow delivery, a process we refer to as landscape hydrologic capacitance. To test this hypothesis, we connected models of soil moisture, upland water table, and wetland stage to simulate hydrology of a low-relief landscape with GIWs, and explored the influences of total wetland area, individual wetland size, climate, and soil texture on water table and base flow variation. Increasing total wetland area and decreasing individual wetland size substantially decreased water table and base flow variation (e.g., reducing base flow standard deviation by as much as 50%). GIWs also decreased the frequency of extremely high and low water tables and base flow deliveries. For the same total wetland area, landscapes with fewer (i.e., larger) wetlands exhibited markedly lower hydrologic capacitance than those with more (i.e., smaller) wetlands, highlighting the importance of small GIWs to regional hydrology. Our results suggest that GIWs buffer dynamics of the surficial aquifer and stream base flow, providing an indirect but significant nexus to the regional hydrologic system.

1. Introduction

Uncertainty about the landscape connectivity and hydrologic functions of geographically isolated wetlands (GIWS; i.e., those surrounded entirely by uplands [*Tiner*, 2003]) has been brought to the policy forefront in the U.S. [*Leibowitz and Nadeau*, 2003] by two recent U.S. Supreme Court rulings (*Solid Waste Agency of Northern Cook County versus U.S. Army Corps*—SWANCC (2001) and *Rapanos versus U.S.* (2006)). These two rulings removed federal protections for GIWs except where a "significant nexus" to navigable or interstate waters exists [*EPA and U.S. Army Corps of Engineers*, 2008]. A significant nexus is defined as a measurable influence to the "chemical, physical, or biological integrity of traditional navigable waters or interstate waters," and has often been considered for jurisdiction of tributaries and wetlands adjacent to drainage features [*EPA and U.S. Army Corps of Engineers*, 2008]. Federal guidance has recognized that GIWs could also fall under jurisdiction if a significant nexus is demonstrated, but stresses the challenges of that demonstration [*EPA and U.S. Army Corps of Engineers*, 2011]. More recently, U.S. Federal authorities proposed new rules that would extend categorical jurisdiction to wetlands adjacent to navigable or interstate waters, but would continue to require case-by-case demonstration of a significant nexus for nonadjacent GIWs [*EPA and U.S. Army Corps of Engineers*, 2014]. With current federal regulation of GIWs predicated on the interpretation and demonstration of a significant nexus, it is imperative to better understand the hydrologic connectivity of GIWs within the landscape [*Leibowitz*, 2003; *Whigham and Jordan*, 2003; *Zedler*, 2003].

Landscape-scale hydrology is driven by the dynamics of storage and flow between surface water and groundwater systems, and connectivity between these systems controls how hydrologic changes in one area impact behavior in others [*Winter*, 1988]. Water exchanges among wetlands, adjacent surface water bodies, and upland systems provide floodwater storage and base flow to regional drainage networks [e.g., *Novitzki*, 1979; *Carter*, 1986; *Ogawa and Male*, 1986], while also attenuating the delivery of nutrients and

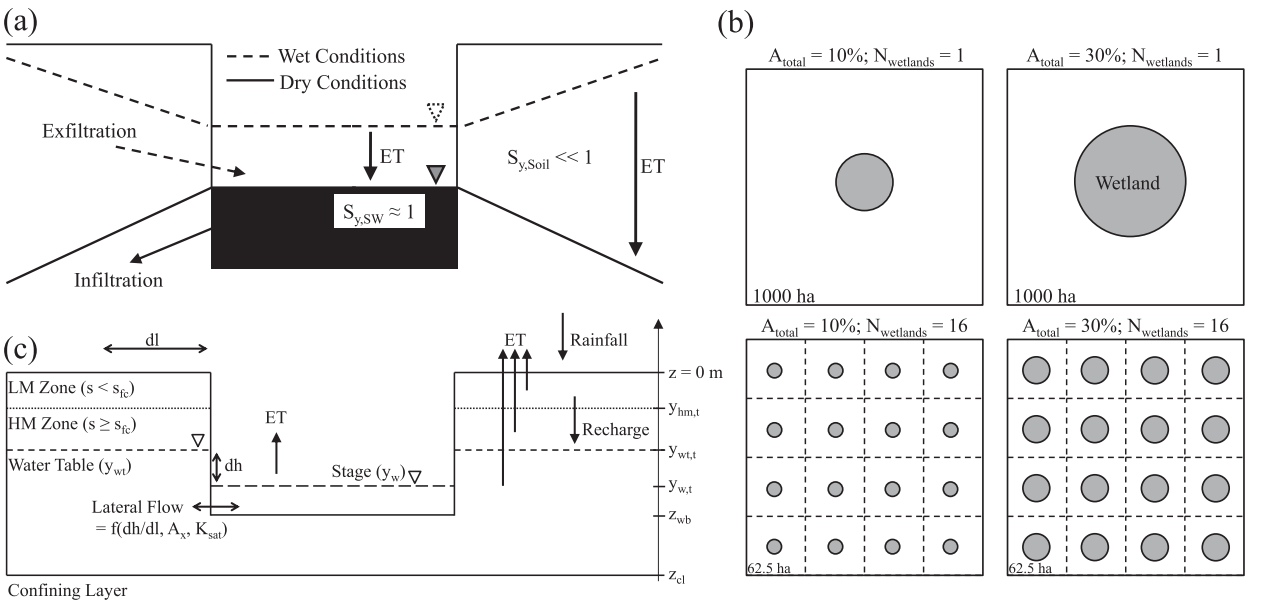

Figure 1. (a) Conceptualization of groundwater exchange between a GIW and its surrounding uplands. Switching between wetland exfiltration and infiltration in response to atmospheric fluxes occurs due to specific yield (S_y) differences between upland and inundated wetlands, with amplified responses to precipitation and evapotranspiration (ET) in upland groundwater levels. (b) Schematic illustrating idealized simulated landscapes with varying combinations of total wetland area (A_{total}) and wetland count ($N_{wetlands}$); we simulated A_{total} ranging from 0 to 40% and $N_{wetlands}$ ranging from 1 to 512. (c) Cross section of idealized wetland and adjacent uplands. Upland soils can be saturated (i.e., y_{wt} = 0 m) or have some unsaturated zone, which we segment into high (HM) and low moisture (LM) zones based on soil moisture.

other contaminants to downstream water bodies [*Udy et al.*, 2006; *Mitsch and Gosselink*, 2007; *Kadlec and Wallace*, 2009]. These services are among the many reasons that wetlands have been conferred protected status (e.g., under Section 404 of the U.S. Federal Clean Water Act and Guidance Document 12 of the European Commission's Water Framework Directive).

While landscape-scale hydrologic functions are well documented in wetlands with obvious surface water connections (e.g., riparian habitats, floodplains, salt marshes, lake littoral wetlands), the role of GIWs is less well known. Several studies have proposed a role for GIWs in reducing runoff and storing floodwaters [*Tiner*, 2003; *Leibowitz and Nadeau*, 2003; *Lane and D'Amico*, 2010]. However, landscapes with GIWs typically have very little relief and are, by virtue of the absence of surface connectivity, located in hydrologically closed basins. Consequently, subsurface flow paths dominate any hydrologic exchange, potentially limiting floodwater storage and release functions. However, GIWs can impact local groundwater dynamics via subsurface exchanges with surrounding uplands [*Winter*, 1988], but the role of these local interactions in regulating regional hydrologic behavior has not been adequately demonstrated.

Wetland-groundwater interactions are complex and time varying, with frequent reversals observed in local flow direction (i.e., wetland discharge to and recharge from the adjacent aquifer) in response to evapotranspiration (ET) and rainfall [*Winter*, 1988, 1999; *Riekerk and Korhnak*, 2000]. In low-relief humid landscapes where GIWs are commonly found, shallow aquifer dynamics are likely to be strongly structured by these hydrologic reversals [*Winter*, 1988]. Sign reversals in hydraulic gradients between GIWs and their surrounding uplands are common in low-relief north Florida landscapes, with commensurate measured rates of infiltration (from the wetland to groundwater) and exfiltration (from the groundwater to the wetland) fluxes [*McLaughlin and Cohen*, 2013, 2014] (though see *Min et al.* [2010] for conditions where reversals have been lost). Flow reversals between exfiltration and infiltration occur in response to specific yield (S_y) differences between aquifers ($S_{y,Soil} \approx 0.1–0.35$ [*Loheide et al.*, 2005]) and surface water ($S_{y,SW}$ often assumed at 1.0 [*Mitsch and Gosselink*, 2007]). On an area basis, S_y is the ratio of output (ET) or input (rain) depth to induced water level change. Lower $S_{y,Soil}$ means that groundwater level responses to both rain and ET are amplified relative to surface water level response (Figure 1a). That is, GIWs most often act as water sinks from the surficial aquifer during wet periods (exfiltration) and water sources (infiltration) during drier times (Figure1a).

Base flow to regional drainage networks is largely controlled by surficial aquifer dynamics [*Winter*, 1999]. It follows that the impacts of GIWs on surficial aquifer dynamics may be propagated to downstream water bodies, even where flow paths never connect water in those wetlands directly to the drainage network. The local sink/source reversal observed in GIWs may buffer surficial aquifer and base flow dynamics, a phenomenon we refer to as landscape hydrologic capacitance, reflecting the predicted ability of areas with high S_y to modulate water level variation given connectivity with areas of lower S_y. Previous research has investigated the influence of $S_{y,Soil}$ on shallow water table dynamics [*Laio et al.*, 2009], as well as stage-varying S_y effects on wetland water levels [*Sumner*, 2007]; however, the integrated effects of spatially varying S_y values between uplands and wetlands have not been explored. In this work, we coupled models of shallow water table and soil moisture dynamics with a wetland water balance model to simulate the effects of total wetland area and individual wetland size on surficial aquifer and base flow dynamics. We further explored how these effects are influenced by soil type and climatic conditions. Our goal was to investigate the nexus between GIWs dispersed across a landscape and the regional water table dynamics that ultimately control stream base flow.

2. Methods

2.1. Model Description

To test the hypothesis that GIWs exert important controls on regional hydrology via interactions with the surficial aquifer system required simulation models of landscapes with varying climate, soil, and wetland attributes (size, density). We integrated existing process-based models of shallow water table [*Laio et al.*, 2009] and soil moisture [*Laio et al.*, 2001] dynamics with a model of wetland hydrology to simulate daily values of wetland stage, upland water table elevation and soil moisture content, and base flow delivery in an idealized landscape ($A = 10$ km^2), in which both the total area and individual size of GIWs were varied (Figure 1b). The model landscape represents low-relief regions where small GIWs exist within a matrix of uplands (e.g., southeastern coastal plain flatwoods/cypress dome systems, prairie pothole region of the northern Great Plains, Nebraska sandhills, Atlantic coastal plain pocosins [*Tiner*, 2003]). Simulated wetlands were cylindrical with bottom elevations denoted by z_{wb} and upland soil elevation as the vertical datum (i.e., upland elevation: $z = 0$; Figure 1c); spatial variation in upland and wetland topography was not considered. The surficial aquifer depth was set based on elevation of the confining layer, denoted by z_{cl} (Figure 1c). For z_{wb} and z_{cl}, we used baseline values of -1.25 and -2.0 m, respectively, and evaluated model sensitivity to these parameters. Total area of GIWs (A_{total}) was varied between 0 and 40% of the land area, with the rest assumed to be homogenous uplands. The total number of GIWs ($N_{wetlands}$) was adjusted by factors of two from 1 to 512 wetlands, with equal local catchment areas for each wetland; adjusting $N_{wetlands}$ yielded different *individual* wetland sizes for a given A_{total} (Figure 1b).

Simulated daily rain and potential evapotranspiration (PET) (section 2.2) were assumed to be spatially constant over the landscape. These atmospheric fluxes drove varying fluctuations in upland water table (section 2.3) and wetland stage (section 2.5) due to S_y differences (Figure 1a), as well as soil moisture storage (section 2.4) and the potential for ET$<$PET in the uplands (based on available soil moisture); these differential responses to climatic drivers created the gradient for local lateral groundwater exchange between wetlands and uplands. Regional groundwater flux across the domain boundary represented base flow to streams and was modeled as a function of landscape mean water table elevation. Both channel and overland flow within the domain boundary were excluded from the model. Vertical flow out of the surficial aquifer was also excluded based on the assumption of a confining layer.

2.2. Climate Simulation

Daily precipitation and PET were simulated for different climatic conditions, allowing us to explore interactive effects between climate, soil type, A_{total}, and $N_{wetlands}$ on water table dynamics. Following *Rodriguez-Iturbe et al.* [1999], daily rainfall (mm) was modeled as Poisson process, $P(\lambda, \alpha)$, with exponentially distributed rainfall depths (mean $= \alpha$) and rainfall frequency λ (i.e., mean number of days between events of $1/\lambda$). We explored values of λ ranging from 0.1 to 0.6 and assumed $\alpha = 10$ mm based on 10 years of climate data from north Florida (Florida Automated Weather Network; http://fawn.ifas.ufl.edu/), yielding a range of mean annual precipitation (MAP) from 365 mm (at $\lambda = 0.1$) to 2190 mm (at $\lambda = 0.6$). PET was modeled as a sine function:

$$PET_t = PET_{min} + \beta^* \sin\left(\pi^* \frac{DOY}{365}\right) \quad (1)$$

Table 1. Soil Parameters Used in Water Table and Soil Moisture Modeling

Parameter	Sand	Sandy Loam	Loam	Source
K_{sat} (m/d)	15.20	3.00	0.60	*Clapp and Hornberger* [1978]
ψ_s (m)	0.12	0.22	0.48	*Clapp and Hornberger* [1978]
s_{fc}	0.44	0.57	0.70	Calculated using *Dingman* [2002]
s_w	0.17	0.26	0.53	Calculated using *Dingman* [2002]
n	0.40	0.44	0.45	*Clapp and Hornberger* [1978]
b	4.05	4.90	5.39	*Clapp and Hornberger* [1978]
$S_{y,Soil}$	0.22	0.19	0.14	Calculated using equation (4)
$y_{c,\ upland}$	−0.45	−0.65	−0.75	*Laio et al.* [2009]
$y_{c,\ wetland}$	−0.30	−0.50	−0.60	*Laio et al.* [2009]

where PET_{min} is the minimum daily PET (assumed to be 0.5 mm), DOY is Julian day of year, and β is a scaling factor, which was varied to simulate annual PET from 600 to 1600 mm yr^{-1}.

2.3. Simulation of Water Table Dynamics

Upland water table elevation (denoted as y_{wt}) was simulated using a shallow water table model developed by *Laio et al*. [2009], which separates the soil profile into three zones (Figure 1c): (1) the saturated zone that extends $|\psi_s|$ above y_{wt}, where ψ_s is the (negative) air entry pressure head (Table 1); (2) the high moisture unsaturated zone, defined as the portion of the soil column above the saturated zone where soil moisture content (s) is at or greater than field capacity (s_{fc}; Table 1); (3) the low moisture zone, where $s < s_{fc}$. The low moisture zone develops only when the saturated zone elevation ($y_{wt} + |\psi_s|$) is at or below a critical depth (y_c; Table 1), where y_c is a function of soil type and rooting depth [see *Laio et al*., 2009]. The water table exerts no influence on the low moisture zone through capillary rise because of extremely low hydraulic conductivities at $s < s_{fc}$ [*Laio et al*., 2009]. The low moisture zone was therefore modeled as a separate system (section 2.4) that influences the high moisture zone and water table through soil water storage capacity (i.e., it serves to reduce water table recharge from rain events).

Upland water table elevation was simulated using a daily water balance equation:

$$y_{wt,t+1} = y_{wt,t} + \frac{dy_{wt}}{dt} \tag{2}$$

$$\frac{dy_{wt}}{dt} = \frac{1}{S_{y,Soil}}\left(R + GW_{local} - ET_{wt} - GW_{bf}\right) \tag{3}$$

where y_{wt} is water table elevation (m), $S_{y,Soil}$ is the upland soil specific yield (dimensionless), R is recharge to the surficial aquifer (m/d) from rain, GW_{local} is local groundwater exchange (m/d) between the surficial aquifer and adjacent wetlands (positive values indicate flow into surficial aquifer), ET_{wt} is the ET flux from the water table, and GW_{bf} is landscape-scale drainage of the surficial aquifer to stream base flow. While $S_{y,Soil}$ varies with water table depth [*Loheide et al*., 2005; *Acharya et al*., 2012], we assumed that topographic variation at the landscape-scale limits this effect; that is, lower $S_{y,Soil}$ in areas of low elevation and higher water tables are modulated by higher $S_{y,Soil}$ in areas of higher elevations. We applied a constant $S_{y,Soil}$ for all water table depths following the equation in *Laio et al*. [2009]:

$$S_{y,soil} = n(1 - s_{fc}) \tag{4}$$

where *n* is porosity and s_{fc} is soil moisture at field capacity (Table 1).

Water table elevations were bounded by confining layer elevation below and the ground surface above (i.e., $z_{cl} \le y_{wt} \le 0.0$; Figure 1c). Water levels at the lower boundary represent complete drying of the surficial aquifer, which can then be rewetted based on R. The upper limit on water table elevations was imposed to reflect that upland flooding (i.e., $y_{wt} > 0$) results in overland flows that rapidly sheds standing water, leaving saturated upland soils (i.e., $y_{wt} = 0$).

Following *Laio et al*. [2009], we assumed the unsaturated hydraulic conductivity in the high moisture zone is large enough to allow instantaneous water redistribution at the daily time step, and that recharge (R) is equal to the water that reaches the high moisture zone. Therefore, when $y_{wt} + |\psi_s| > y_c$ (i.e., no low moisture zone exists), R equals rain depth, and when $y_{wt} + |\psi_s| \le y_c$, R equals rain depth less the available soil storage in the low moisture zone (section 2.4). Local groundwater exchange (m^3/d) between wetlands and uplands was determined using Darcy's equation driven by hydraulic gradients (dh) between upland water table and wetland stage (section 2.5), a flow length (dl) equal to the distance between upland centroid and wetland edge, hydraulic saturated conductivity (K_{sat}; Table 1), and the appropriate cross-sectional area for exchange (A_x) (Figure 1c). A_x was calculated using the elevation difference between wetland stage and the confining layer (Figure 1c) along with wetland circumference (Figure 1b). Note that increasing A_{total} and/or

$N_{wetlands}$ increases A_x (by increasing total wetland perimeter) and decreases dl, both of which increase local groundwater flow rates. Local groundwater volumetric exchange (m^3/d) was divided by upland area to determine GW_{local} (m/d).

ET fluxes from the high moisture zone were assumed to be instantaneously satisfied by capillary rise from the water table [*Laio et al*., 2009]. Therefore, ET_{wt} was the sum of root uptake and soil evaporation from both the water table and high moisture zone. When $y_{wt} + |\psi_s| > y_c$, ET_{wt} equals PET (i.e., evaporative demand is fully met). However, when $y_{wt} + |\psi_s| \leq y_c$, root uptake from both the high moisture zone and water table is reduced because some percentage of total root biomass is in the low moisture zone. In this case, ET_{wt} was modeled as an exponential decline from PET [*Laio et al*., 2009], assuming an exponential distribution of root biomass [*Schenk and Jackson*, 2002]:

$$ET_{wt} = PET \times e^{y_{hm}/RD} \tag{5}$$

where y_{hm} is the elevation of the upper boundary of the high moisture zone (section 2.4) and RD is the geometric mean of rooting depth. We used a baseline mean rooting depth of 0.4 m, which is representative of uplands in coastal plain flatwoods ecosystems [*Van Rees and Comerford*, 1986], and evaluated model sensitivity to this parameter.

Landscape-scale drainage of the surficial aquifer (GW_{bf}) was calculated to determine base flow rates to downstream surface waters. Base flow was modeled as a linear function of y_{wt} following the approach of *Tamea et al*. [2010], assuming a constant boundary head equal to the elevation of the confining layer (z_{cl}; Figure 1c), which represents the bottom elevation of a proximal stream:

$$GW_{bf} = k \times (y_{wt} - z_{cl}) \tag{6}$$

To parameterize k, we iteratively selected values to yield observed ratios of annual base flow to MAP in sandy watersheds of the southeastern coastal plain (e.g., base flow/MAP = 0.10) [*Sun et al*., 2002]. For other soil types, k values were adjusted in proportion to differences in K_{sat} (Table 1). GW_{bf} and total landscape area were used to calculate base flow as volumetric flow rates (l/s); variation in base flow as well as in the water table elevation (y_{wt}) was the principal model output considered in response to varying wetland attributes, climate, and soil conditions.

2.4. Simulation of Soil Moisture in the Low Moisture Zone

When $y_{wt} + |\psi_s| \leq y_c$, a low moisture zone develops where $s < s_{fc}$ (Figure 1c). Following *Laio et al*. [2009], the boundary elevation (y_{hm}) between the high and low moisture zones was modeled as a function of y_{wt}, y_c, RD, ψ_s, and s_{fc} (Table 1; see *Laio et al*. [2009] for model details). A soil moisture model similar to *Laio et al*. [2001] was applied to simulate low moisture zone dynamics with a volume-balance equation determining average s over the low moisture zone profile:

$$s_{t+1} = s_t + \frac{ds}{dt} \tag{7}$$

$$n|y_{hm}|\frac{ds}{dt} = P - L(s) - ET_{lm}(s) \tag{8}$$

where *n* is porosity (Table 1), $|y_{hm}|$ is the absolute value of upper boundary of the high moisture zone (i.e., the thickness of the low moisture zone; Figure 1c), P is rain (m/d), L is leakage (m/d) to the high moisture zone, and ET_{lm} is the ET flux from the low moisture zone; both L and ET_{lm} are a function of time-varying soil moisture content (s_t). As before, unsaturated hydraulic conductivities at $s > s_{fc}$ are assumed large enough for instantaneous water redistribution. Therefore, vadose storage in the low moisture zone is equal to $n * |y_{hm}| * (s_{fc} - s)$, and any excess water infiltrates to the high moisture zone through leakage (L). As such, P – L is vadose storage, with L recharging the water table (i.e., R in equation (3) when $y_{wt} + |\psi_s| \leq y_c$).

When $y_{wt} + |\psi_s| \leq y_c$, $ET_{wt} < PET$ (section 2.3), and the remaining atmospheric demand (PET-ET_{wt}) was applied as *potential* ET uptake from the low moisture zone (PET_{lm}). ET_{lm} was determined as a function of both PET_{lm} and the water available to meet this demand (s). Similar to *Laio* [2006], we assumed ET_{lm} decreases linearly from PET_{lm} at $s = s_{fc}$ to zero at the permanent wilting point ($s = s_w$; Table 1) with:

$$ET_{lm} = PET_{lm}\frac{(s - s_w)}{(s_{fc} - s_w)} \quad (9)$$

2.5. Simulation of Wetland Stage Dynamics

Like the upland water table, wetland stage was simulated using a daily water balance equation:

$$y_{w,t+1} = y_{w,t} + \frac{dy_w}{dt} \quad (10)$$

$$\frac{dy_w}{dt} = \frac{1}{S_{y,SW}}(P + GW_{local} - ET_w) \quad (11)$$

where y_w is wetland stage elevation (m), $S_{y,SW}$ is specific yield of surface water (1.0, dimensionless), P is rain (m/d), GW_{local} is local groundwater exchange between the wetland and surrounding surficial aquifer (m/d; positive values of GW_{local} indicate wetland exfiltration; negative values indicate infiltration), and ET_w is assumed equal to PET (m/d). We previously demonstrated that S_y of a flooded wetland can fall below unity as stage decreases [*McLaughlin and Cohen*, 2014]; here, where we assumed cylindrical wetlands, we exclude this effect and assumed that $S_{y,SW} = 1.0$ except where stage falls below the wetland bottom. Local groundwater exchange (m^3/d), calculated previously (section 2.3), was divided by wetland area and reversed in sign to determine GW_{local} in m/d. When wetland stage fell below the wetland bottom elevation (z_{wb}; Figure 1c), the water table below the wetland was calculated using the methodology and soil parameters (Table 1) used for the upland water table (section 2.3) and soil moisture dynamics (section 2.4); however, we used a lower mean rooting depth based on the shallow rooting profile of many wetland plants [*Blom and Voesenek*, 1996]. We applied a baseline geometric mean rooting depth of 0.1 m and evaluated model sensitivity to a range of values.

2.6. Combined Model

Simulated daily fluctuations in s, y_{wt}, y_w, and base flow were integrated via vadose storage effects on water table recharge, ET_{wt} control on ET_{lm}, lateral exchange between wetlands and uplands, and water table regulation of base flow. The fully coupled model was run using a range of climate parameters (λ from 0.1 to 0.6 and annual ET from 600 to 1600 mm), three soil types (sand, sandy loam, and loam), total wetland areas (A_{total}) ranging from 0 to 40%, and wetland count ($N_{wetlands}$) from 1 to 512 within the 10 km^2 domain. Because wetland stage and water table elevation were sensitive to the timing and magnitude of simulated rain and ET, the model was run for 1000 years for each parameter configuration, at which point variance in wetland stage, water table elevation, and base flow stabilized. We evaluated the effects of A_{total} and $N_{wetlands}$ on landscape hydrologic capacitance by quantifying changes in the mean, standard deviation, and frequency distributions of daily upland water table elevation and base flow between simulations with and without wetlands. We also performed a sensitivity analysis by adjusting several model parameters (upland and wetland rooting depths, wetland elevation (z_{wb}), and confining layer elevation (z_{cl})) that are poorly constrained by empirical values in the literature or exhibit variation across regions. Finally, model sensitivity to soil-specific parameters was explored by comparing three different soil types.

3. Results

Model simulations representing Florida flatwood soils (sand in Table 1) and climate ($\alpha = 10$ mm, $\lambda = 0.35$, and annual PET = 1450 mm) were performed with different configurations of A_{total} and individual wetland size (via adjusting $N_{wetlands}$). Comparing elevations of y_w, y_{wt}, and y_{hm} over five simulated years (shown for a landscape with $A_{total} = 30\%$ and $N_{wetlands} = 256$ in Figure 2a) illustrates the dampened response of wetland stage to atmospheric fluxes compared to upland water table elevations. Differential responses to rainfall and ET between the two systems result from higher S_y in the inundated wetland than in the adjacent upland (i.e., $S_{y,Soil} < S_{y,SW}$), which causes switching in the direction of groundwater exchange (Figure 2b). The resulting buffering effect on y_{wt}, enumerated as the relative change in water table standard deviation (SD_{wt}) between landscapes with and without wetlands, is a function of both A_{total} and $N_{wetlands}$ (i.e., wetland size) (Figure 3). Increasing A_{total} while keeping $N_{wetlands}$ constant lowers SD_{wt} compared to a landscape with no wetlands (shown for $N_{wetlands} = 256$ in Figure 3a). Similarly, maintaining constant wetland area ($A_{total} = 30\%$) but changing $N_{wetlands}$ (i.e., few large wetlands versus numerous small wetlands) reveals a strong influence of smaller wetlands on water table regulation (Figure 3b). In particular, we note that the

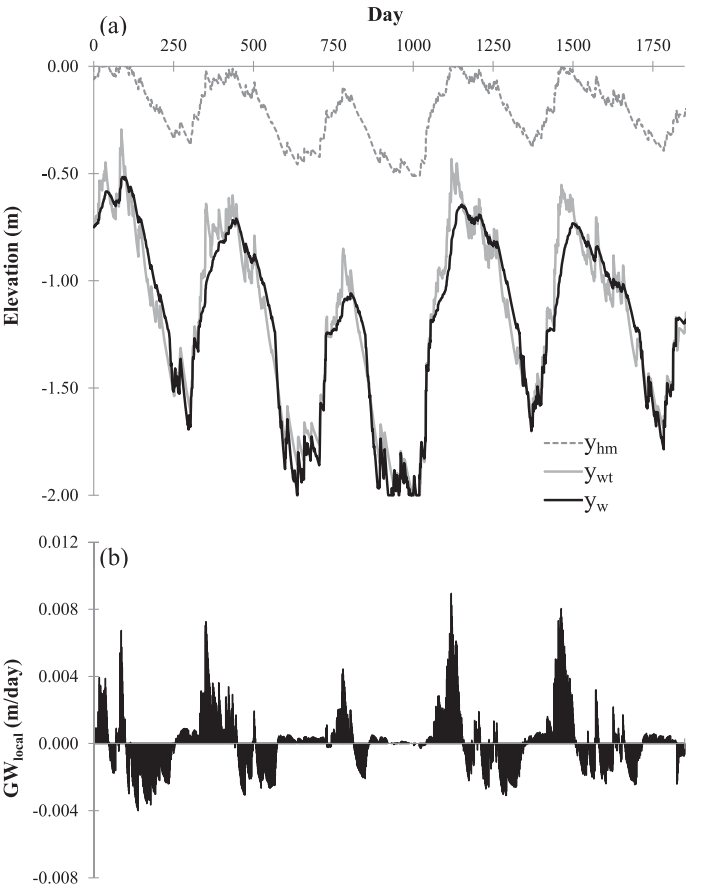

Figure 2. (a) Wetland stage (y_w), water table elevation (y_{wt}), and high moisture zone elevation (y_{hm}) with time in response to rainfall and ET with A_{total} = 30% and $N_{wetlands}$ =256. (b) Reversals in hydraulic gradient ($y_{wt} - y_w$) result in switching between wetland exfiltration (positive GW_{local}) and infiltration (negative GW_{local}).

change in SD_{wt} occurs sharply when total wetland area is comprised of a greater number of smaller wetlands; this effect levels off at ~256 wetlands (i.e., wetland size = 1.2 ha). The high moisture vadose zone elevation (y_{hm}) showed similar decreases in standard deviation with increasing A_{total} and/or $N_{wetlands}$ (data not shown) as expected since the soil moisture profile is influenced by the underlying water table (section 2.4; Figure 2a).

While increasing either A_{total} or $N_{wetlands}$ reduces SD_{wt}, the mean water table elevation remains constant (Figures 3a and 3b). Histograms of changes in water table depths vis-à-vis no wetland conditions illustrate that increasing A_{total} or $N_{wetlands}$ decreases the frequency of shallow and deep water tables, while increasing the frequency of water tables at intermediate elevations (Figures 3c and 3d). The mechanism that enables this buffering role of GIWs is that increasing A_{total} and/or $N_{wetlands}$ increases the magnitude of wetland-groundwater exchange. For example, increasing $N_{wetlands}$ from 64 to 256 wetlands while keeping A_{total} constant at 30% more than doubles the mean volume exchanged between wetlands and uplands across the landscape (1861 versus 3932 m^3/d; data not shown).

As expected, the buffering effect of GIWs on water table variation extends to landscape-scale base flow delivery (Figure 4). Compared to wetland influences on SD_{wt}, increasing A_{total} or $N_{wetlands}$ results in even greater reductions in base flow standard deviation (SD_{bf}) relative to no wetland conditions (Figures 4a and 4b). Increasing A_{total} or $N_{wetlands}$ also creates modest decreases in mean base flow (Figures 4a and 4b) due to the maintenance of higher ET rates in wetlands (vis-à-vis uplands) when the water table is deep; however, the frequencies of both extreme low and extreme high base flow events are reduced in landscapes with wetlands relative to the no wetland condition (Figures 4c and 4d).

The relative effects and trade-offs between A_{total} and $N_{wetlands}$ on water table and base flow dynamics obtained from 72 simulations (A_{total} varied between 5 and 40% in 5% steps, $N_{wetlands}$ varied from 1 to 512 by factors of 2) suggest that the buffering effect of wetlands is largest at the highest values of A_{total} and $N_{wetlands}$; this is shown as a relative change in SD_{bf} vis-à-vis no wetland conditions (ΔSD_{bf}; Figure 5). However, intermediate buffering effects can be obtained by varying configurations of A_{total} and $N_{wetlands}$. For example, ΔSD_{bf} of approximately −15% is possible with A_{total} = 20% if the wetlands are small ($N_{wetlands}$ = 512), but twice as much wetland area (A_{total} = 40%) is required to achieve the same buffering effect with larger wetlands ($N_{wetlands}$ = 64). Increasing A_{total} has a relatively constant effect between $N_{wetlands}$ of 128 and 512; however, this effect substantially decreases with lower wetland densities and becomes negligible at $N_{wetlands} < 16$.

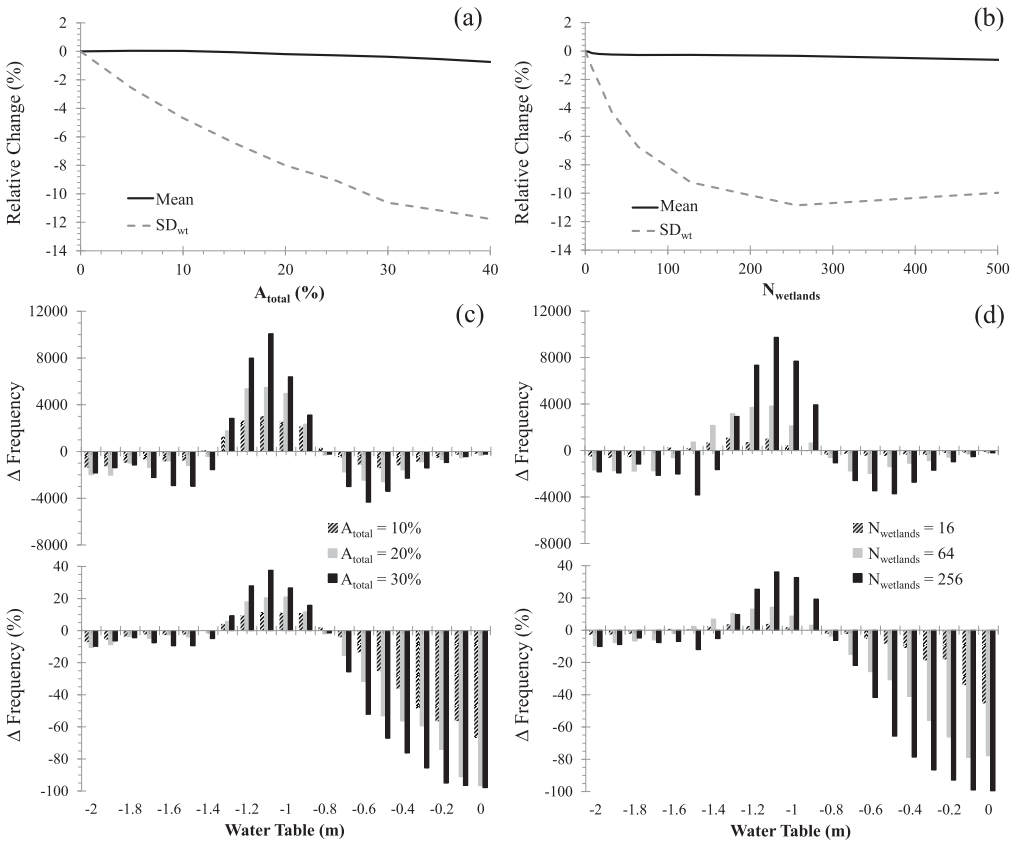

Figure 3. The standard deviation (SD_{wt}) of daily water table elevation declines relative to no wetland conditions (shown as % change), while the mean remains constant, for (a) increasing A_{total} but with constant $N_{wetlands} = 256$ and (b) increasing $N_{wetlands}$ keeping A_{total} at 30%. Changes in frequencies (absolute and relative) of water table depths relative to no wetland conditions show that increasing (c) A_{total} or (d) $N_{wetlands}$, while keeping the other constant ($N_{wetlands} = 256$ and $A_{total} = 30\%$, respectively), reduces the frequency of high and low water table elevations and increases the frequency of intermediate elevations.

Analysis of model sensitivity to poorly constrained parameters (upland and wetland rooting depths, wetland elevation, and confining layer elevation) suggests significant sensitivity to wetland elevation and confining layer elevation, moderate sensitivity to upland rooting depth, and little sensitivity to wetland rooting depth (Figure 6). Sensitivity to wetland elevation and confining layer elevation is driven largely by changes to system geometry; these parameters define the cross-sectional area for groundwater exchange and affect the proportion of vadose storage in the low soil moisture zone. Despite sensitivity to these site-specific parameters, observed effects of A_{total} and $N_{wetlands}$ on ΔSD_{bf} were retained across the full range of parameter values, suggesting the magnitude of the predicted effect is modestly sensitive to parameter values, but not its direction.

Buffering effects from GIWs varied with climate and soil type. Simulations with constant A_{total} (30%) and $N_{wetlands}$ (256) but varying MAP (via changes to λ), annual PET, and soil type (sand, sandy loam, and loam) illustrate the marked influence of climate and soil type on base flow buffering (Figure 7). In sandy soils, buffering effects were largest (i.e., ΔSD_{bf} approaches −50%) for the most humid (i.e., high MAP, low PET) conditions (Figure 7a), while for sandy loam and loam, effects were maximized where MAP and PET are relatively balanced (i.e., ΔSD_{bf} approaches −30 and −15% along the diagonal of the ET-rainfall plane in Figures 7b and 7c, respectively).

Base flow buffering was largest in the coarsest soil (sand; Figure 7a) compared with finer soils (sandy loam and loam; Figures 7b and 7c). Soil type affects two parameters that control the local groundwater reversal behavior central to the buffering mechanism: $S_{y,Soil}$ and K_{sat}. Finer soils have lower S_y (Table 1), which amplifies difference in water level responsiveness between wetlands and uplands. However, fine-grained soils also have lower values of K_{sat} (Table 1), which limit the equilibration of water levels via groundwater exchange. In a landscape with $A_{total} = 30\%$, $N_{wetlands} = 256$, and moderate climate ($\lambda = 0.3$, yielding a MAP of 1095 mm, and PET = 1200), mean local groundwater exchange between wetland and uplands was nearly 300% greater with

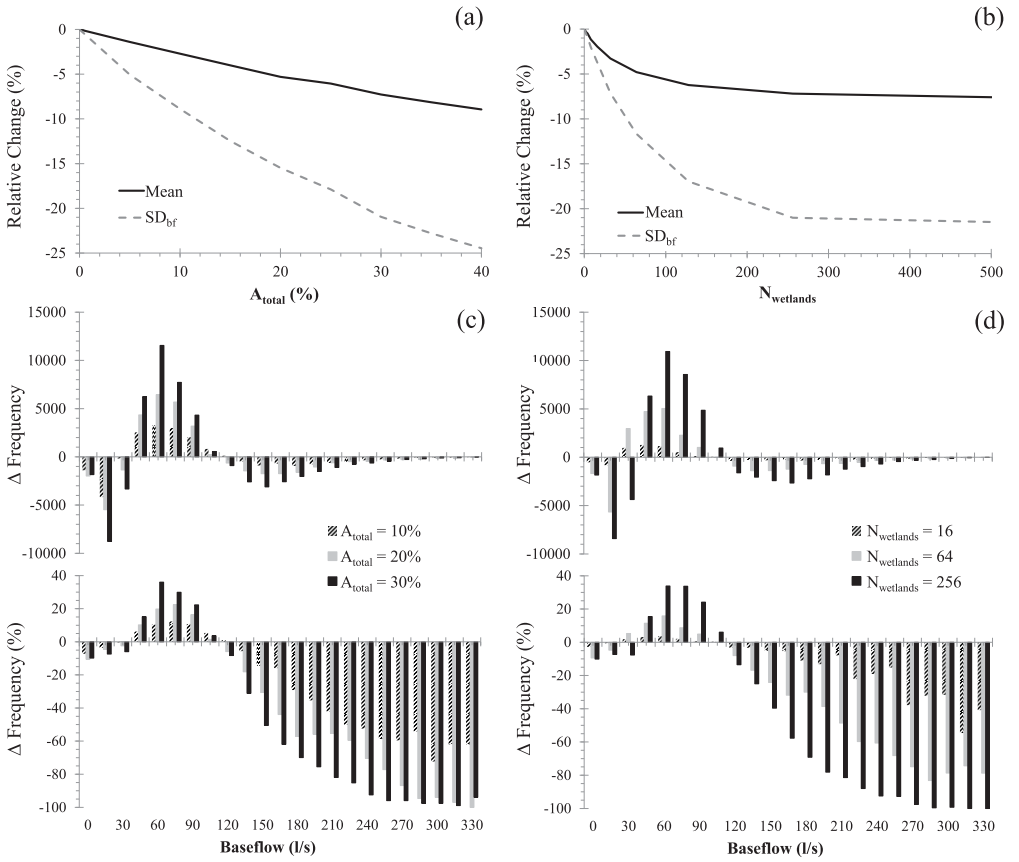

Figure 4. Both the mean and standard deviation (SD_{bf}) of daily base flow decline relative to no wetland conditions (shown as % change) for (a) increasing A_{total} but with constant $N_{wetlands} = 256$ and (b) increasing $N_{wetlands}$ keeping A_{total} at 30%. Changes in frequencies (absolute and relative) of base flow relative to no wetland conditions show that increasing (c) A_{total} or (d) $N_{wetlands}$, while keeping the other constant ($N_{wetlands} = 256$ and $A_{total} = 30\%$, respectively), reduces the frequency of high and low flow events and increases the frequency of intermediate flows.

sandy soils (3724 m^3/d) compared to loamy soils (1021 m^3/d). Thus, reduced exchange capacity at low K_{sat} outweighs the effects of reduced S_y, leading to reduced water table buffering and thus ΔSD_{bf} in fine-grained soils (Figure 7c). In even finer soils (e.g., clayey loam and clay), groundwater fluxes became negligible and wetland effects on water table and base flow dynamics were not apparent (data not shown).

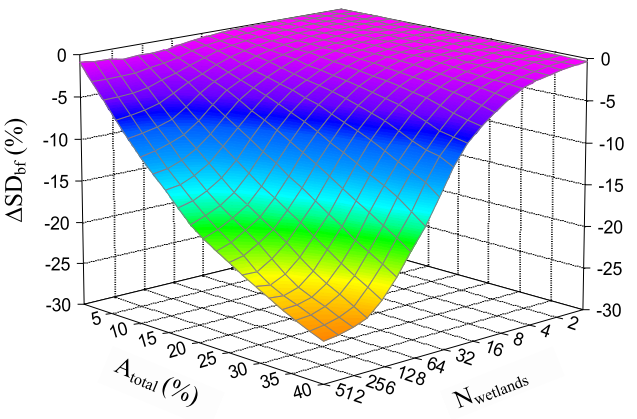

Figure 5. Combined effects of A_{total} and $N_{wetlands}$ on changes in base flow variation (ΔSD_{bf} (%)) demonstrate that the largest impacts occur at high A_{total} and $N_{wetlands}$, and that effects of increasing A_{total} are greatly reduced when $N_{wetlands} < 32$. Note log scale on $N_{wetlands}$ axis.

4. Discussion

Hydrologic functions associated with wetlands (e.g., flood abatement, groundwater recharge, and base flow supply) are often assumed to be generally applicable to all wetlands, although empirical evidence counters such a broad generalization [*Bullock and Acreman*, 2003]. Connectivity between wetlands and drainage networks determines how wetlands impact downstream flow and water quality, suggesting that these functions are strongly dependent on

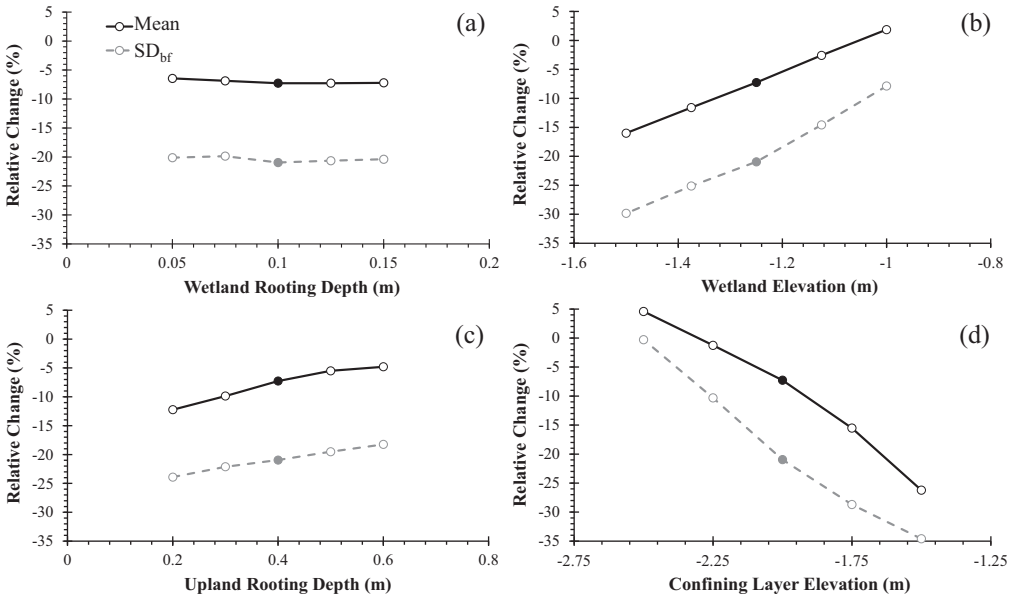

Figure 6. Sensitivity analysis for impacts of (a) wetland rooting depth, (b) wetland elevation, (c) upland rooting depth, and (d) confining layer elevation on relative changes (%) in mean and standard deviation (SD_{bf}) of base flow compared to no wetland conditions (A_{total} = 30%, $N_{wetlands}$ = 256). While the magnitude of wetland effects is sensitive to some parameter values, the direction of those effects (i.e., buffering base flow) is not. Closed circles denote baseline values.

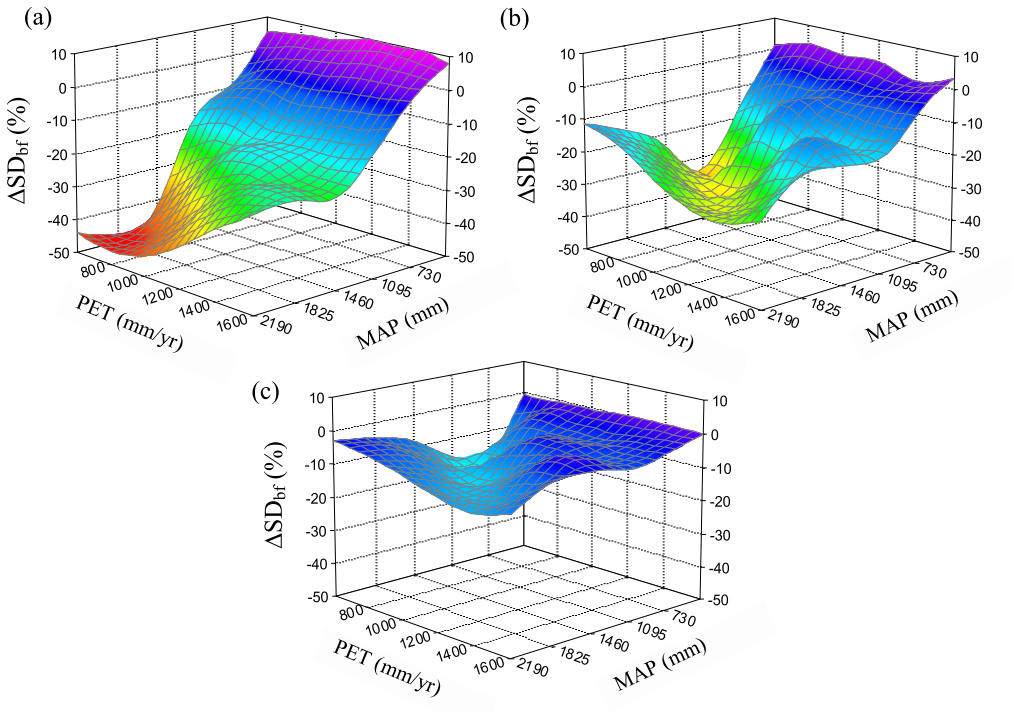

Figure 7. Interactions between mean annual precipitation (MAP) and PET determine the magnitude of wetland effects on base flow variation (ΔSD_{bf} (%)) with A_{total} = 30% and $N_{wetlands}$ = 256. Soil type also controls the magnitude of these effects, shown here for (a) sand, (b) sandy loam, and (c) loam.

wetland type and setting. While direct surface water connections (e.g., between floodplains and streams, or between littoral wetlands and lakes) create clear and significant connectivity, such direct links are not always present, particularly in GIWs [*Winter and LaBaugh*, 2003]. Given the federal wetland regulatory implications (in the U.S.), the hydrologic connectivity and function of GIWs are of particular relevance. This study suggests that GIWs regulate regional aquifer dynamics through local groundwater exchange, conferring hydrological services to downstream water bodies even where a direct surface water connection may be absent. The aquifer buffering capacity created by GIWs has direct and important impacts on base flow volume and consistency in streams and other systems connected to the regional groundwater system.

The hydrological service of water table and base flow buffering, a function we refer to as landscape hydrologic capacitance, arises when wetlands alternate between water sinks and sources. This capacitance is created and maintained by S_y differences between wetlands and their adjacent uplands and by rapid water exchange between them (i.e., high K_{sat}). The magnitude of the landscape hydrologic capacitance function increases with total wetland area (A_{total}); as expected, the degree to which wetland-groundwater exchange is increased and water table variation is buffered (i.e., reductions in SD_{wt}) increases as wetlands occupy a larger proportion of the landscape (Figure 3a). The buffering effect of wetland area on the surficial aquifer propagates to downstream base flow; indeed, base flow buffering was even higher (i.e., greater reductions in SD_{bf} than in SD_{wt}; Figure 4a). Increasing A_{total} dramatically lowered the frequencies of high and low water table elevations (Figure 3c), and the frequencies of high and low base flow events (Figure 4c). Together, these model predictions suggest that the area of GIWs exerts important controls on regional hydrology, ranging from buffering upland water table and soil moisture dynamics to regulating base flow behavior in the regional drainage network.

While increasing A_{total} increases landscape hydrologic capacitance, decreasing the size of individual GIWs (via increasing the number of wetlands; $N_{wetlands}$) at a constant A_{total} exerts an equal or even greater effect. Reversals in the sign of hydraulic gradients between wetlands and uplands demonstrate the changing gradient for wetland-upland groundwater exchange (Figure 2); however, the *total volume* of this local groundwater exchange is controlled by wetland perimeter, not area. As such, the landscape hydrologic capacitance given a fixed wetland area increases with smaller individual wetland size and thus perimeter for exchange (Figures 3b, 3d, 4b, and 4d). These results emphasize the disproportionately important role that small GIWs play in providing hydrologic capacitance; indeed, the buffering effect of increasing A_{total} is negligible when wetlands are large (e.g., $N_{wetlands} \leq 16$; Figures 4b and 5). The strong effect of wetland size on hydrologic capacitance raises concerns about preferential losses of small, spatially distributed GIWs, and the preferential protection (and even creation) of larger wetlands within compensatory mitigation programs. Numerous studies [*Zedler*, 1996; *Bonds and Pompe*, 2003; *Bendor*, 2009] have assessed the structural and functional benefits (e.g., larger buffers, higher success rates) and costs (e.g., inability to replace similar wetland types, loss of species and habitat diversity) of mitigating the losses of small wetlands by enhancing or constructing large wetlands; this study suggests that large wetlands fail to provide the same landscape-scale hydrologic buffering services as provided by small GIWs.

There are several important functions to both upland ecosystems and downstream waters that accrue from the observed surficial aquifer and base flow buffering. By reducing the frequency of deep water tables and low base flow during periods of low rainfall, GIWs have obvious and important implications to terrestrial productivity (i.e., reduced water stress) and aquatic habitat (e.g., maintenance of dry-season refugia and migration pathways). Similarly, by lowering the frequency of high water table and base flow conditions, GIWs reduce downstream vulnerability to overland flow generation and associated hazards, including stream bank erosion and sediment transport. Finally, regular reversals in the direction of upland-wetland groundwater exchange enhances solute exchange through wetland soils, very likely increasing biogeochemical reaction rates and thus improving water quality.

While GIWs reduce base flow and water table variation, and have little effect on mean water table elevation, they do appear to lower mean base flow (Figures 4a and 4b). This occurs because ET rates in upland areas are substantially reduced under low water table conditions, whereas wetlands maintain high ET rates even when they are not inundated because their root zone is closer to the water table. As such, wetlands experience steeper ET-induced water level declines (vis-à-vis uplands) and serve as landscape hydrologic sinks during extreme dry conditions (Figure 2). This flux from the upland water table to wetlands is balanced by a concomitant reduction in base flow, allowing mean water table elevations to be maintained while mean

base flow is reduced. We note, however, that this decline in mean base flow is modest compared with reductions in SD_{bf} (Figures 4a and 4b). The primacy of reduced variation over reduced mean flow explains why the frequency of extreme low base flow events can be reduced despite a decline in the overall mean base flow (Figure 4). Moreover, since wetlands are able to maintain higher ET under dry conditions relative to upland areas, they act as productivity and water use "hot spots" in the landscape [*Bullock and Acreman*, 2003], conferring other regional benefits related to ET (e.g., productivity, carbon sequestration, and microclimate regulation) [*McLaughlin and Cohen*, 2013].

Landscape hydrologic capacitance requires that the volume of local groundwater exchange between uplands and wetlands be large, which means that the effect is most pronounced in settings with coarser upland soils that have higher hydraulic conductivity (K_{sat}). Given the same head gradient, more conductive soils also have greater capacity to deliver base flow from the surficial aquifer. Simulations with sandy soils (at a constant $A_{total} = 30\%$ and $N_{wetlands} = 256$) resulted in reductions in SD_{bf} of up to 48%, compared to only 34% and 18% in sandy loam and loamy soils, respectively (Figure 7). This means that GIWs in regions with coarser soils (e.g., Atlantic coastal plain, Nebraska sandhills) will have a larger impact on landscape hydrologic capacitance than in settings with fine soils (e.g., clayey loam), which exhibited minimal water table and base flow buffering (data not shown). In those settings, surface water processes (ponding and runoff) control water budgets, not local groundwater exchange, which may mean that wetlands are more regularly connected via surface pathways. As such, GIWs in regions with finer soils may confer other hydrologic functions (e.g., runoff storage and slow groundwater recharge) that were not modeled here.

Climate also influences the hydrologic capacitance function of GIWs. In sandy soils (at a constant $A_{total} = 30\%$ and $N_{wetlands} = 256$), the largest base flow buffering effects (ΔSD_{bf} between -40 and -50%) were realized when MAP was highest and PET was lowest (i.e., MAP:PET >1.8); however, substantial buffering (ΔSD_{bf} between -15 and -25%) occurred for more moderate climates (i.e., $1.0 <$ MAP:PET <1.5; Figure 7a). These climate conditions exist in the southeastern and northern Atlantic coastal plains (MAP/PET $\sim$1.0) [*Dingman*, 2002], where GIWs (e.g., cypress domes, pocosins, Carolina Bays, Delmarva potholes, coastal plain ponds, alluvial depressional swamps) are common [*Tiner*, 2003], as well as the Great Lakes region (MAP/PET $\geq$1.0 [*Dingman*, 2002]) and its associated wetlands (e.g., alvars, kettle-holes). For finer soils, effects were maximized (ΔSD_{bf} of -30 and -15% in sandy loam and loam, respectively) in moderate climates (i.e., MAP/PET ratios from $\sim$1.0 to 1.8; Figures 7b and 7c). In contrast, the buffering effect of GIWs was substantially lower in drier climates with low rainfall and moderate to high PET (i.e., in semiarid to arid regions with MAP/PET <0.5—Nebraska sandhills, west coast vernal pools, southwestern playas [*Dingman*, 2002]).

To isolate the role of GIWs on water table and base flow dynamics and explore controls on the magnitude of the hydrologic capacitance function, our model purposely neglected certain hydrologic fluxes, including surface drainage within and across watersheds, surface runoff, and vertical leakage. While neglecting these fluxes limits comparison with empirical data, recent evidence [*McLaughlin and Cohen*, 2013] supports both the behavior and magnitude of simulated upland-wetland groundwater exchanges that create hydrologic capacitance. Specifically, our model yielded regular reversals between wetland exfiltration and infiltration, as well as local groundwater exchange rates, commensurate with field observations [*McLaughlin and Cohen*, 2013] when simulating values for wetland area ($A_{total} = 30\%$) [*Marois and Ewel*, 1983] and individual wetland size ($N_{wetlands} = 256$ or approximately 1 ha) [*Ewel and Wickenheiser*, 1988] similar to those observed in sandy, low-relief landscapes in north Florida and across the southeastern coastal plain more broadly. While this cannot confirm the magnitude of wetland buffering in other regions with different MAP/PET ratios, soil textures, and wetland-upland configurations, it does provide confirmation that the predicted effects occur and are empirically detectable.

An additional simplification inherent to our model is the assumption of cylindrical wetlands, which simplifies the geometric relationships describing the area for upland-wetland groundwater exchange and allowed us to characterize landscape-scale buffering as a function of total area and number/size of GIWs. The actual bathymetry of GIWs is often bowl shaped, which creates a relationship between wetland stage and inundated area that is a function of basin topography. Assuming cylindrical basins overestimates the buffering effect of more bowl-shaped basins since the total inundated area (with $S_y \sim 1.0$), and thus the area that provides hydrologic capacitance, decreases with stage. This effect is likely small in GIWs with relatively flat-bottomed topography (e.g., playa wetlands [*Tang et al.*, 2013] and prairie potholes [*Shaw et al.*, 2012]). However, where basin shapes are more convex (e.g., coastal plain ponds [*Schneider*, 1994] and cypress domes

[*Watson et al.*, 1990]) overall landscape hydrologic capacitance would decrease as a function of inundated area (e.g., a landscape with $A_{total} = 40\%$ would begin to behave more similarly to a landscape with lower total area as wetland stage declines).

Waters are considered under federal jurisdiction "if they, either alone or in combination with similarly situated waters in the region, significantly affect the chemical, physical, or biological integrity of traditional navigable waters or interstate waters" [*EPA and U.S. Army Corps of Engineers*, 2011]. Demonstrating downstream effects from cumulative losses of a wetland class extends jurisdiction to an *individual wetland within that class* [*Leibowitz*, 2003] (emphasis added). Our simulations strongly suggest that GIWs exert important controls on regional hydrology, and that loss of this class of wetlands would have discernible downstream impacts. This finding is underscored by the observation that smaller GIWs, for which protections are the weakest, provide greatly enhanced water table and base flow buffering capacity at the landscape-scale vis-à-vis larger wetlands with same total wetland area.

Taken together with previous empirical observations of groundwater flow reversals in GIWs [*McLaughlin and Cohen*, 2013], the modeling results presented here demonstrate that a significant "hydraulic" nexus exists between GIWs and distant water bodies via influences to the regional water table, and ultimately its regulation of downstream base flow. The use here of the word hydraulic emphasizes that the role these GIWs play in buffering surficial aquifer dynamics and downstream base flow is realized even where water in these systems may never physically reach downstream systems. We conclude that there is a high likelihood of a significant but indirect nexus between GIWs and navigable waters.

Acknowledgments
This work was supported by the Environmental Protection Agency under grant EPA#L CD-95417909-0. We appreciate insights from Scott Leibowitz, Nandita Basu, and Charles Lane who commented on early drafts of this work. All data and code used in this work can be obtained from the authors.

References

Acharya, S., J. W. Jawitz, and R. S. Mylavarapu (2012), Analytical expressions for drainable and fillable porosity of phreatic aquifers under vertical fluxes from evapotranspiration and recharge, *Water Resour. Res.*, *48*, W11526, doi:10.1029/2012WR012043.

Bendor, T. (2009), A dynamic analysis of the wetland mitigation process and its effects on no net loss policy, *Landscape Urban Plann.*, *89*(1), 17–27.

Blom, C. W., and L. A. Voesenek (1996), Flooding: The survival strategies of plants, *Trends Ecol. Evol.*, *11*(7), 290–295.

Bonds, M. H., and J. J. Pompe (2003), Calculating wetland mitigation banking credits: Adjusting for wetland function and location, *Nat. Resour. J.*, *43*, 961–977.

Bullock, A., and M. Acreman (2003), The role of wetlands in the hydrological cycle, *Hydrol. Earth Syst. Sci.*, *7*, 358–389.

Carter, V. (1986), An overview of the hydrologic concerns related to wetlands in the United States, *Can. J. Bot.*, *64*, 364–374.

Clapp, R. B., and R. B. Hornberger (1978), Empirical equations for some soil hydraulic properties, *Water Resour. Res.*, *14*, 601–604.

Dingman, L. (2002), *Physical Hydrology*, 2nd ed., Prentice Hall, Upper Saddle River, N. J.

EPA and U.S. Army Corps of Engineers (2008), Clean Water Act Jurisdiction following the U.S. Supreme Court's decision in Rapanos versus United States and Carabell versus United States, U.S. Environmental Protection Agency and Army Corps of Engineers Guidance Memorandum.

EPA and U.S. Army Corps of Engineers (2011), Draft guidance on identifying waters protected by the Clean Water Act, U.S. Environmental Protection Agency and Army Corps of Engineers Draft Guidance Document.

EPA and U.S. Army Corps of Engineers (2014), Proposed rule on definition of "Waters of the United States" under the Clean Water Act, U.S. Environmental Protection Agency and Army Corps of Engineers Draft Guidance Document.

Ewel, K. C., and L. P. Wickenheiser (1988), Effect of swamp size on growth rates of cypress (Taxodium distichum) trees, *Am. Midland Nat.*, *120*(2), 362–370.

Kadlec, R. H., and S. Wallace (2009), *Treatment Wetlands*, 2nd ed., CRC press, Boca Raton, Fla.

Laio, F. (2006), A vertically extended stochastic model of soil moisture in the root zone, *Water Resour. Res.*, *42*, W02406, doi:10.1029/2005WR004502.

Laio, F., A. Porporato, L. Ridolfi, and I. Rodriguez-Iturbe (2001), Plants in water-controlled ecosystems: Active role in hydrologic processes and response to water stress II. Probabilistic soil moisture dynamics, *Adv. Water Resour.*, *24*, 707–723.

Laio, F., S. Tamea, L. Ridolfi, P. D. D'Odorico, and I. Rodriguez-Iturbe (2009), Ecohydrology of groundwater-dependent ecosystems: 1. Stochastic water table dynamics, *Water Resour. Res.*, *45*, W05419, doi:10.1029/2008WR007292.

Lane, C. R., and E. D'Amico (2010), Calculating the ecosystem service of water storage in isolated wetlands using LiDAR in north central Florida, USA, *Wetlands*, *30*, 967–977, doi:10.1007/s13157-010-0085-z.

Leibowitz, S. G. (2003), Isolated wetlands and their functions: An ecological perspective, *Wetlands*, *23*, 517–531.

Leibowitz, S. G., and T. Nadeau (2003), Isolated wetlands: State-of-the-science and future directions, *Wetlands*, *23*, 663–684.

Loheide, S. P., II, J. J. Butler Jr., and S. M. Gorelick (2005), Estimation of groundwater consumption by phreatophytes using diurnal water table fluctuations: A saturated-unsaturated flow assessment, *Water Resour. Res.*, *41*, W07030, doi:10.1029/2005WR003942.

Marois, K. C., and K. C. Ewel (1983), Natural and management-related variation in cypress domes, *For. Sci.*, *29*, 627–640.

McLaughlin, D. L., and M. J. Cohen (2013), Realizing ecosystem services: Wetland hydrologic function along a gradient of ecological condition, *Ecol. Appl.*, *23*(7), 1619–1631.

McLaughlin, D. L., and M. J. Cohen (2014), Ecosystem specific yield for estimating evapotranspiration and groundwater exchange from diel surface water variation, *Hydrol. Processes*, *28*, 1495–1506, doi:10.1002/hyp.9672.

Min, J., D. B. Perkins, and J. W. Jawitz (2010), Wetland-groundwater interactions in subtropical depressional wetlands, *Wetlands*, *30*, 991–1106, doi:10.1007/s13157-010-0043-9.

Mitsch, W. J., and J. G. Gosselink (2007), *Wetlands*, 4th ed., John Wiley, Hoboken, N. J.

Novitzki, R. P. (1979), Hydrologic characteristics of Wisconsin's wetlands and their influence on floods, stream flow, and sediment, in *Wetland Functions and Values: The State of Our Understanding*, edited by P. E. Greeson, J. R. Clark, and J. E. Clark, pp. 1–674, Am. Water Resour. Assoc., Minneapolis, Minn.

Ogawa, H., and J. W. Male (1986), Simulating the flood mitigation role of wetlands, *J. Water Resour. Plann. Manage.*, *112*(1), 114–128.
Riekerk, H., and L. V. Korhnak (2000), The hydrology of cypress wetlands in Florida pine flatwoods, *Wetlands*, *20*, 448–460.
Rodriguez-Iturbe, I., A. Porporato, L. Ridolfi, V. Isham, and D. R. Cox (1999), Probabilistic modelling of water balance at a point: The role of climate, soil and vegetation, *Proc. R. Soc. London, Ser. A*, *455*, 3789–3805.
Schenk, H. J., and R. B. Jackson (2002), The global biogeography of roots, *Ecol. Monogr.*, *72*, 311–328.
Schneider, R. (1994), The role of hydrologic regime in maintaining rare plant communities of New York's coastal plain pondshores, *Biol. Conserv.*, *68*(3), 253–260.
Shaw, D. A., A. Pietroniro, and L. W. Martz (2012), Topographic analysis for the prairie pothole region of Western Canada, *Hydrol. Processes*, *27*, 3105–3114, doi:10.1002/hyp.9409.
Sumner, D. M. (2007), Effects of capillarity and microtopography on wetland specific yield, *Wetlands*, *27*, 693–701.
Sun, G., S. G. McNulty, D. M. Amatya, R. W. Skaggs, L. W. Swift Jr., J. P. Shepard, and H. Riekerk (2002), A comparison of the watershed hydrology of coastal forested wetlands and the mountainous uplands in Southern US, *J. Hydrol.*, *263*, 92–104.
Tamea, S., R. Muneepeerakul, F. Laio, L. Ridolfi, and I. Rodriguez-Iturbe (2010), Stochastic description of water table fluctuations in wetlands, *Geophys. Res. Lett.*, *37*, L06403, doi:1029/2009GL041633.
Tang, Z., R. Li, X. Li, W. Jiang, and A. Hirsh (2013), Capturing LiDAR-derived hydrologic spatial parameters to evaluate playa wetlands, *J. Am. Water Resour. Assoc.*, *50*(1), 234–245, doi:10.1111/jawr.12125.
Tiner, R. W. (2003), Geographically isolated wetlands of the United States, *Wetlands*, *23*, 494–516.
Udy, J. W., C. S. Fellows, M. E. Bartkow, S. E. Bunn, J. E. Clapcott, and B. D. Harch (2006), Measures of nutrient processes as indicators of stream ecosystem health, *Hydrobiologia*, *572*(1), 89–102.
Van Rees, K. C., and N. B. Comerford (1986), Vertical root distribution and strontium uptake of a slash pine stand on a Florida spodosol, *Soil Sci. Soc. Am. J.*, *50*, 1042–1046.
Watson, J., D. Stedje, M. Barcelo, and M. Stewart (1990), Hydrogeologic investigation of cypress dome wetlands in well field areas north of Tampa, Florida, paper presented at Focus Eastern Conference, Natl. Water Well Assoc., Dublin, Ohio.
Whigham, D. F., and T. E. Jordan (2003), Isolated wetlands and water quality, *Wetlands*, *23*(3), 541–549.
Winter, T. C. (1988), A conceptual framework for assessing cumulative impacts on the hydrology of nontidal wetlands, *Environ. Manage.*, *12*, 605–620.
Winter, T. C. (1999), Relation of streams, lakes, and wetlands to groundwater flow systems, *Hydrogeol. J.*, *7*, 28–45.
Winter, T. C. and J. W. LaBaugh (2003), Hydrologic considerations in defining isolated wetlands, *Wetlands*, *23*, 532–540.
Zedler, J. B. (1996), Ecological issues in wetland mitigation: An introduction to the forum, *Ecol. Appl.*, *6*, 33–37.
Zedler, P. H. (2003), Vernal pools and the concept of "isolated wetlands," *Wetlands*, *23*(3), 597–607.